Behavioral/Systems/Cognitive

Orexin Directly Excites Orexin Neurons through Orexin 2 Receptor

Akihiro Yamanaka,[1,2,3]* Sawako Tabuchi,[1,2,3]* Tomomi Tsunematsu,[1,2,3] Yugo Fukazawa,[2,3] and Makoto Tominaga[1,2,3]

[1]Section of Cell Signaling, Okazaki Institute for Integrative Bioscience, National Institute of Natural Sciences, Okazaki 444-8787, Japan, [2]National Institute for Physiological Sciences, National Institute of Natural Sciences, Okazaki 444-8585, Japan, and [3]Department of Physiological Sciences, The Graduate University for Advanced Studies, Okazaki 444-8787, Japan

Orexin neurons (hypocretin neurons) have a critical role in the regulation of sleep/wakefulness, especially in the maintenance of arousal. Here, we revealed that orexin neurons are directly and indirectly activated by orexin via the orexin 2 receptor (OX2R). Orexin B (1 μM) induced depolarization in orexin neurons, which was still observed in the presence of TTX (1 μM), AP-5 (50 μM), and CNQX (20 μM). In addition, orexin B induced inward currents in the presence of TTX, suggesting a direct activation of orexin neurons. Although orexin B application induced depolarization in orexin neurons of OX1R knock-out mice at comparable levels to wild-type mice, the observation that orexin B failed to depolarize orexin neurons in the OX2R knock-out mice suggested that OX2R was a primary receptor for this response. Moreover, immunoelectron microscopic analyses revealed direct contacts among orexin neurons, which exhibited structural similarities to the glutamatergic synapses. Together, these results suggest that orexin neurons form a positive-feedback circuit through indirect and direct pathways, which results in the preservation of the orexin neuron network at a high activity level and/or for a longer period. Therefore, the activation of orexin neurons through OX2R might have an important role in the maintenance of arousal.

Introduction

Orexin A (hypocretin-1) and orexin B (hypocretin-2) are produced exclusively by a population of neurons in the lateral hypothalamic area (de Lecea et al., 1998; Sakurai et al., 1998). The actions of the two orexins are mediated via two G-protein-coupled receptors, namely the orexin 1 receptor (OX1R) and orexin 2 receptor (OX2R) (Sakurai et al., 1998). OX1R has an ~100-fold higher affinity for orexin A than for orexin B. On the other hand, OX2R has an almost equal affinity for both peptides. Animals that lack the prepro-orexin gene, OX2R gene, or orexin neurons showed narcolepsy-like behavior such as fragmentation of sleep/wakefulness, direct transitions from wake to rapid eye movement (REM) sleep, and the sudden loss of muscle tone while still awake (cataplexy) (Chemelli et al., 1999; Lin et al., 1999; Hara et al., 2001; Willie et al., 2003). However, OX1R null mice showed mild or almost no abnormality in the regulation of sleep/wakefulness, suggesting that the orexin signal through OX2R has a critical role in the regulation of sleep/wakefulness, especially in the maintenance of arousal. The expression pattern of orexin receptors matches the afferent projections of orexin neurons throughout the brain. OX2R mRNA has been shown to be prominent in the cerebral cortex, septal nuclei, hippocampus, and hypothalamic nuclei, including the histaminergic tuberomammillary nucleus (TMN) (Marcus et al., 2001). Among these brain regions, the TMN is thought to be the center for the site of action of orexin-induced arousal, because histaminergic TMN neurons are implicated in arousal (Lin et al., 1988; Monti, 1993). The TMN neurons fire tonically during wakefulness (Steininger et al., 1999) and are activated by orexin via OX2R (Bayer et al., 2001; Eriksson et al., 2001; Yamanaka et al., 2002). In addition, the effect of orexin on arousal was not observed in histamine 1 receptor knock-out ($H1^{-/-}$) mice (Huang et al., 2001). However, histidine decarboxylase knock-out ($HDC^{-/-}$) mice, $H1^{-/-}$ mice, and $OX1R^{-/-}$;$H1^{-/-}$ double knock-out mice did not show severe abnormalities in sleep/wakefulness (Anaclet et al., 2009; Hondo et al., 2010), suggesting that downstream pathways of OX2R, other than the histaminergic system, are critical for sleep/wakefulness regulation.

In this study, we revealed that orexin neurons are directly and indirectly activated by orexin via the OX2R. We showed by using an immunoelectron microscope that orexin neurons are directly innervated by orexin neurons. In addition, orexin indirectly activates orexin neurons by increasing spontaneous EPSCs (sEPSCs) in orexin neurons. This indirect activation was also mediated primarily through the OX2R. Although orexin neurons in the $OX1R^{-/-}$ mice showed comparable activation with wild-type orexin neurons by orexin B application, the orexin neurons in the $OX2R^{-/-}$ mice completely failed to respond to orexin B. These results suggest that orexin neurons form a positive-feedback circuit between orexin neurons. This circuitry might have a role in maintaining a high level of activity of orexin neurons while animals are awake.

Received April 25, 2010; revised June 14, 2010; accepted July 1, 2010.

This study was supported by the Japan Science and Technology Agency PRESTO program, a Grant-in-Aid for Young Scientist (A), Scientific Research on Priority Areas (Integrative Brain Research), the Comprehensive Brain Science Network from the Ministry of Education, Culture, Sports, Science, and Technology of Japan (A.Y., Y.F.), a Japan Society for Promotion of Science postdoctoral fellowship (T.T.), and the Nakajima Foundation (A.Y.). We thank Drs. K. Nakada, K. F. Tanaka, and M. Maruyama for technical advice.

*A.Y. and S.T. contributed equally to this work.

Correspondence should be addressed to Dr. Akihiro Yamanaka, National Institute for Physiological Sciences, National Institute of Natural Sciences, Okazaki 444-8787, Japan. E-mail: yamank@nips.ac.jp.

DOI:10.1523/JNEUROSCI.2120-10.2010

 0270-6474/10/3012642-11$15.00/0

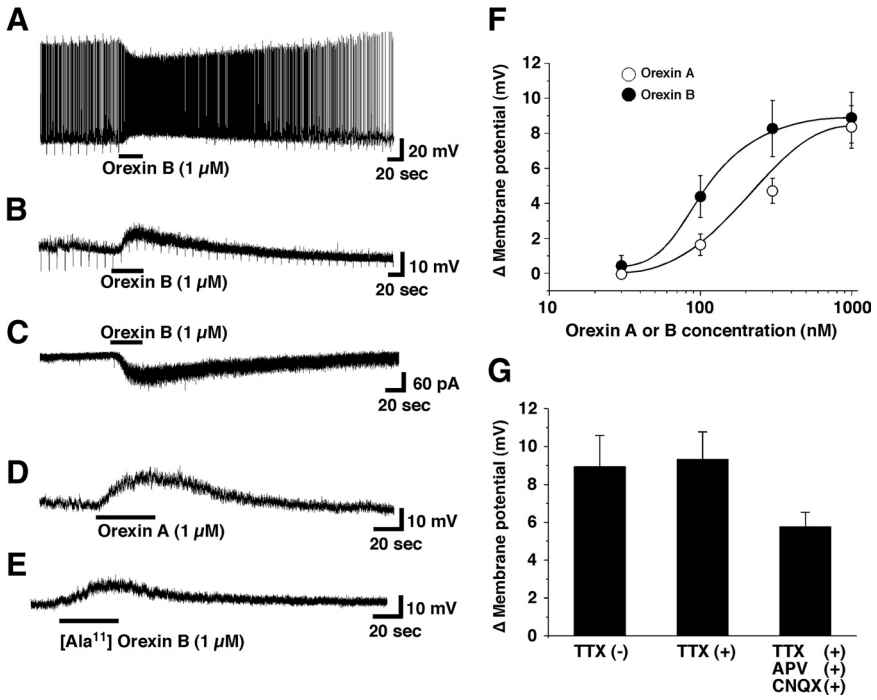

Figure 1. Orexin neurons are directly activated by orexins. ***A***, Under current-clamp mode, application of orexin B (1 μM) induced depolarization and an increase in firing in orexin neurons. ***B***, In the presence of TTX (1 μM), orexin B (1 μM) induced depolarization in orexin neurons. In ***A*** and ***B***, input resistance was monitored by the amplitude of electrotonic potentials generated by the injection of a rectangular wave current pulse (−20 pA, 500 ms, 0.1 Hz). ***C***, Under voltage-clamp mode holding at −60 mV, application of orexin B (1 μM) induced an inward current in orexin neurons in the presence of TTX (1 μM). ***D***, ***E***, Orexin A (1 μM) (***D***) or [Ala ^{11}]-orexin B (1 μM) (***E***) application induced depolarization in the presence of TTX. ***F***, Responses induced by orexin A (EC_{50} = 352 nM, n = 6–22) and orexin B (EC_{50} = 101 nM, n = 6–15) were concentration dependent. ***G***, Bar graph shows orexin B induced depolarization in the presence of TTX (1 μM), APV (50 μM), and CNQX (20 μM) (n = 7–15). Orexin A, orexin B, and [Ala ^{11}]-orexin B were locally applied during the period represented by the bars. Values are mean ± SEM (n = 6–22).

Materials and Methods

Animal usage. All experimental procedures involving animals were approved by the Institutional Animal Care and Use Committee of the National Institutes of Natural Sciences and were in accordance with National Institutes of Health guidelines. All efforts were made to minimize animal suffering or discomfort and reduce the number of animals used.

Animals. Transgenic mice that express enhanced green fluorescent protein (EGFP) in orexin neurons (*orexin/EGFP* mice) under the control of the human prepro-orexin promoter were used for the experiments (Sakurai et al., 1999; Yamanaka et al., 2003a,b). *Orexin/EGFP* mice (BDF1; C57BL/6J:DBA = 50:50) were bred with *OX1R* $^{-/-}$ (C57BL/6J) or *OX2R* $^{-/-}$ (C57BL/6J) mice to generate *orexin/EGFP*;*OX1R* $^{+/-}$ or *orexin/EGFP*;*OX2R* $^{+/-}$ mice (*OX1R* $^{-/-}$ mice and *OX2R* $^{-/-}$ mice were kindly provided by Dr. M. Yanagisawa at the University of Texas Southwestern, Dallas, TX). The mice, which have the *orexin/EGFP* transgene and an alternative orexin receptor gene allele that is hetero, were bred with each other to generate *orexin/EGFP*; *OX1R* $^{-/-}$ (*OE-OX1R* $^{-/-}$; C57BL/6J:DBA = 75:25) or *orexin/EGFP*; *OX2R* $^{-/-}$ (*OE-OX2R* $^{-/-}$; C57BL/6J:DBA = 75:25) mice. These mice express EGFP in orexin neurons and systemically lack the alternative orexin receptor gene (OX1R or OX2R).

We used transgenic mice whose orexin neurons expressed a light-activated chloride pump halorhodopsin (haloR) fused with GFP (*orexin/haloR* mice) for immunoelectron microscopic analyses. *Orexin/haloR* mice were bred with *orexin/EGFP* mice to obtain *orexin/EGFP*; *orexin/haloR* double transgenic mice. Both EGFP and haloR::GFP were expressed in the orexin neurons of these transgenic mice.

Electrophysiological recordings. *OE-OX1R* $^{-/-}$ and *OE-OX2R* $^{-/-}$ mice (male and female) were used for whole-cell slice patch recordings. The slices were transferred to a recording chamber (RC-27L, Warner Instrument) on a fluorescence microscope stage (BX51WI; Olympus). Neurons with EGFP fluorescence were subjected to electrophysiological recording. The fluorescence microscope was equipped with an infrared camera (C2741-79; Hamamatsu Photonics) for infrared differential interference contrast imaging and a charge-coupled device (CCD) camera (IK-TU51CU, Olympus) for fluorescent imaging. Each image was displayed separately on a monitor (Gawin; EIZO) and saved on a Macintosh computer (Apple) through a graphic converter (PIX-MPTV; Pixcela). Recordings were performed with an Axopatch 200B amplifier (Molecular Devices) using a borosilicate pipette (GC150-10; Harvard Apparatus) prepared by a micropipette puller (P-97; Sutter Instruments) filled with intracellular solution (4–10 MΩ), consisting of the following (in mM): 138 K-gluconate, 8 NaCl, 10 HEPES, 0.2 EGTA-Na_3, 2 MgATP, and 0.5 Na_2GTP, pH 7.3 with KOH. The osmolarity of the solutions was checked by a vapor pressure osmometer (model 5520; Wescor) and found to be 280–290 and 320–330 mOsm/L for the internal and external solutions, respectively. The liquid junction potential of the patch pipette and perfused extracellular solution was estimated to be 3.9 mV and was applied to the data. Recording pipettes were under positive pressure while advancing toward individual cells in the slice. Tight seals on the order of 1.0–1.5 GΩ were made by negative pressure. The membrane patch was then ruptured by suction. The series resistance during recording was 10–25 MΩ. The reference electrode was an Ag-AgCl pellet immersed in bath solution. During recordings, cells were superfused with extracellular solution at a rate of 1.6 ml/min using a peristaltic pump (Dynamax; Rainin). sEPSCs and spontaneous IPSCs (sIPSCs) were recorded in orexin neurons under whole-cell voltage-clamp mode at holding potentials of −20 and −60 mV, respectively. sEPSCs were recorded by using a K-gluconate-based pipette solution containing the sodium channel blocker QX-314 (1 mM) to inhibit action potentials in the recording neuron and with picrotoxin (400 μM) in the bath solution. sIPSCs were recorded by using a K-gluconate-based pipette solution containing QX-314 (1 mM) in the presence of DL-2-amino-5-phosphono-pentanoic acid (AP-5) (50 μM) and 6-cyano-7-nitroquinoxaline-2,3-dione (CNQX) (20 μM) in the bath solution. The frequency and amplitude of sEPSCs or sIPSCs were measured by using Minianalysis software (version 6.0.3, Synaptosoft), and only those events with amplitudes >10 pA were used in the analysis.

The output signal was low-pass filtered at 5 kHz and digitized at 10 kHz. Data were recorded on a computer through a Digidata 1322A A/D converter using pClamp software (version 10; Molecular Devices). Traces were processed for presentation by using Origin 8.1 (OriginLab) and Canvas X (ACD Systems) software.

Microscopic investigation of associations among orexin neurons. Six-week-old *orexin/EGFP*;*orexin/HaloR* double transgenic mice (male) were deeply anesthetized with sodium pentobarbital (50 mg/kg body weight, i.p.). They were perfused with 25 mM PBS for 1 min followed by a fixative containing 4% paraformaldehyde (TAAB), 0.05% glutaraldehyde (Nacalai Tesque), and 15% saturated picric acid in 0.1 M phosphate buffer (PB, pH 7.4) for 12 min. Coronal sections containing the lateral hypothalamic area were cut from the fixed brain by a slicer (VT-1000S; Leica) at a thickness of 50 μm. These sections were washed twice in PB, cryoprotected in a solution containing 25% sucrose and 10% glycerol in 20 mM PB, and freeze-thawed with liquid nitrogen. After several washes in PB and 50 mM Tris-HCl-buffered saline (TBS, pH 7.4), the sections were incubated with blocking solution containing 20% normal goat serum

(NGS) in TBS for 30 min and then for 48 h at 4°C with an anti-EGFP rabbit polyclonal antibody (1:800; Invitrogen) and/or an anti-orexin rabbit antibody 1:2000 (Nambu et al., 1999) in 50 mM TBS containing 1% NGS. After several washes in TBS, the sections were incubated overnight with biotinylated goat anti-rabbit IgG antibody (1:100; Vector Laboratories) diluted in 1% NGS in TBS at 4°C. The sections were washed with TBS and reacted with avidin-biotin peroxidase complex (1:100 ABC-Elite; Vector Laboratories) diluted in TBS for 2 h at room temperature. After washing three times in TBS, the sections were washed once in 50 mM Tris-HCl buffer, pH 7.4, and then incubated in 0.05% 3,3′-diaminobenzidine tetrahydrochloride (DAB; Dojindo) solution (containing 50 mM Tris-HCl buffer and 0.003% hydrogen peroxide) at room temperature until the appropriate signal was achieved. The DAB reaction was terminated by several incubations in PB, and then the sections were fixed with 0.5% OsO_4 for 40 min, stained with uranyl acetate (1% in distilled water) for 35 min, dehydrated, and flat-embedded in Durcupan resin (ACM; Fluka/Sigma-Aldrich). We observed the flat-mounted sections with light microscopy by using a BX50 microscope (Olympus) equipped with a DP70 CCD camera (Olympus). Section areas containing immunopositive cells were trimmed out from the sections and re-embedded in Durcupan resin blocks. Ultrathin sections at thickness of 70 nm were prepared with an ultramicrotome (Ultracut T; Leica) and observed with a transmission electron microscope (Tecnai10; FEI). Digital images were captured by a MegaView III CCD camera (Olympus) and processed with iTEM software (Olympus) and Illustrator CS3 (Adobe) for image analysis and preparation of figures, respectively. Three-dimensional reconstructions of the neuronal profiles were performed with serially sectioned ultrathin sections by using Reconstruct (freeware) provided through the synapse web (Fiala, 2005).

Drugs. Orexin A (Bachem), orexin B (Peptide Institute), and [Ala^{11}, D-Leu^{15}]-orexin B ([Ala^{11}]-orexin B) (Tocris Bioscience) were dissolved in extracellular solution and applied by local application through a fine tube (100 μm diameter) positioned near the recording neurons. CNQX, AP-5 (Sigma), picrotoxin (PTX), and tetrodotoxin (TTX) (Wako) were dissolved in extracellular solution and applied by bath application. BAPTA (Dojindo) was dissolved in the pipette solution.

Statistical analyses. Data were analyzed by one-way ANOVA followed by Fisher's protected least significant difference test using the Stat View 4.5 software package (Abacus Concepts). The Kolmogorov–Smirnov statistical test was used to measure cumulative probability of synaptic events. Probability (p) values <0.05 were considered statistically significant.

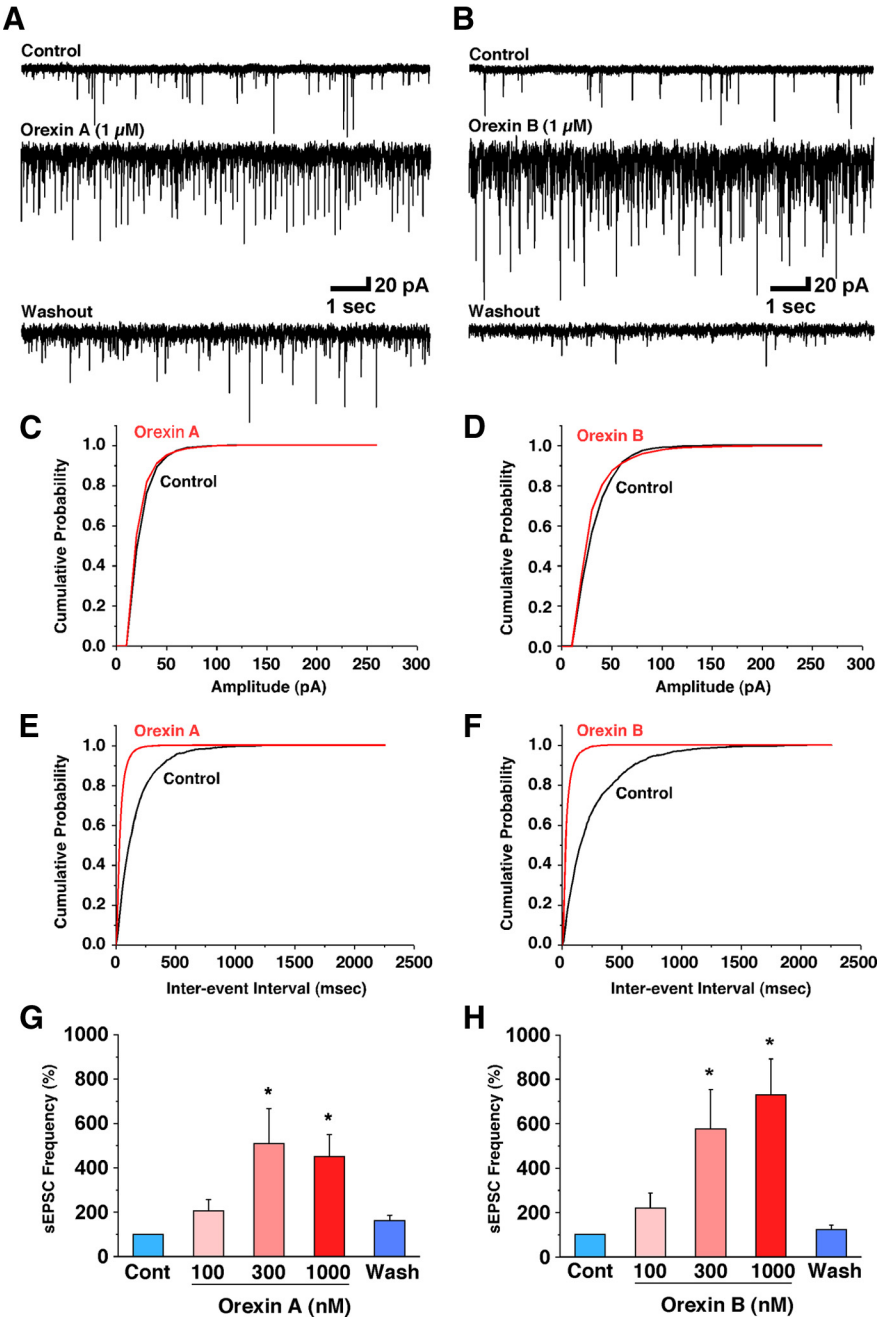

Figure 2. Both orexin A and B increased the sEPSCs in orexin neurons. ***A***, ***B***, sEPSCs were recorded in the presence of PTX (400 μM) at a holding potential of −60 mV. Orexin A and B (1 μM) increased sEPSCs. ***C***, ***D***, Orexin A and B (1 μM) did not change the sEPSC amplitude. ***E***, ***F***, Orexin A and B (1 μM) shortened the interevent interval. ***G***, ***H***, Bar graphs show that orexin A (***G***) and orexin B (***H***) increased sEPSCs in a concentration-dependent manner. Cont, Control. Wash, Washout. *$p < 0.05$ versus control. Values are mean ± SEM ($n = 7$–12).

Results

Orexin neurons are activated by orexin

We studied the effect of orexin on the activity of orexin neurons by using transgenic mouse models. Under current-clamp mode, the local application of orexin B significantly depolarized the membrane potential and increased firing frequency (Fig. 1*A*). The local application of vehicle (extracellular solution) induced slight depolarization (0.2 ± 0.2 mV, used as a vehicle control, $n = 7$). Orexin A and B induced depolarization in a concentration-dependent manner in the presence of TTX, suggesting that orexin directly activates orexin neurons (Fig. 1*B*,*D*,*F*). Orexin B (1 μM)- and orexin A (1 μM)-induced depolarization in the presence of TTX was 9.3 ± 1.5 mV ($n = 15$, $p < 0.0001$ vs control) and 8.8 ± 1.2 mV ($n = 22$, $p = 0.001$, vs control), respectively (Fig. 1*F*). Orexin B-induced depolarization of orexin neurons in *orexin/EGFP* mice was not inhibited by chelating intracellular Ca^{2+} ions. Orexin B (1 μM)-induced depolarization in the presence of

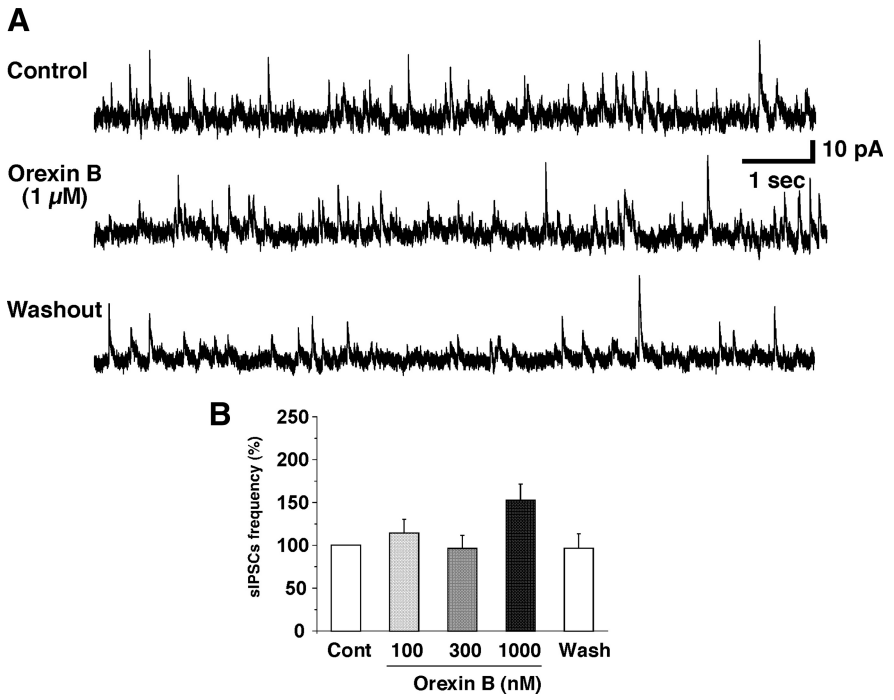

Figure 3. The effect of orexin B on the sIPSCs in orexin neurons. sIPSCs were recorded in the presence of AP5 (50 μM) and CNQX (20 μM) at a holding potential of −10 mV. ***A***, Orexin B (1 μM) showed little effect on sIPSCs. ***B***, Bar graph summarizes sIPSC frequency data from ***A***. Cont, Control. Wash, Washout. *$p < 0.05$ versus control. Values are mean ± SEM ($n = 7–8$).

BAPTA (10 mM) in the pipette solution was 5.8 ± 0.8 mV ($n = 6$, $p = 0.14$, not significantly different vs in the presence of TTX). Approximately 77% of orexin neurons tested were depolarized by orexin (112 of 146) in the *orexin/EGFP* mice. A small number of orexin neurons showed no response or faint depolarization (23%, 34 of 146). The EC_{50} of orexin A- and B-induced depolarizations were 352.7 nM ($n = 6–22$) and 100.9 nM ($n = 6–15$), respectively. Under voltage clamp at a holding potential of −60 mV, orexin B induced inward currents in orexin neurons (Fig. 1*C*). Orexin B (1 μM) induced 30.9 ± 4.6 pA ($n = 6$) inward currents. To further confirm the direct effect induced by orexin B, we used the glutamate receptor antagonists APV and CNQX. In the presence of TTX, APV, and CNQX, orexin B (1 μM) still induced significant depolarization (5.8 ± 0.8 mV, $n = 7$, $p = 0.017$ vs control) (Fig. 1*G*). These results strongly suggest that orexin directly activates orexin neurons. The orexin B-induced depolarization was comparable to orexin A, suggesting the involvement of OX2R in orexin-induced activation of orexin neurons because OX2R has equal affinity for orexin A and B (Sakurai et al., 1998). In addition, [Ala^{11}]-orexin B, an OX2R-selective agonist (Asahi et al., 2003), induced depolarization in the presence of TTX (8.25 ± 1.6 mV, $n = 6$, $p = 0.0001$ vs control), suggesting that OX2R is involved in orexin-induced depolarization in orexin neurons (Fig. 1*E*).

Orexin indirectly activates orexin neurons through the activation of glutamatergic neurons

Li et al. (2002) showed that orexin neurons are indirectly activated by orexin through the activation of glutamatergic neurons. To confirm this indirect activation, sEPSCs were recorded from orexin neurons in the presence of PTX (400 μM) at a holding potential of −60 mV. In this recording condition, sEPSCs are recorded as inward currents. These inward currents were completely abolished by adding AP5 (50 μM) and CNQX (20 μM) in the extracellular solution (data not shown). Both orexin A and B application increased sEPSC frequency in a concentration-dependent manner (Fig. 2*A*,*G*, a nd *B*,*H*, respectively). Although the interevent interval was shortened by orexin A (1 μM) or orexin B (1 μM) application, the amplitude was not affected [Kolmogorov–Smirnov test: amplitude, orexin A ($p = 0.9$), orexin B ($p = 0.2$); interevent interval, orexin A ($p < 0.001$), orexin B ($p = 0.001$) (Fig. 2*C*,*E* or *D*,*F*)]. Orexin A application of 100, 300, and 1000 nM induced 205.8 ± 50.4% ($n = 7$, $p = 0.33$), 508 ± 157.4% ($n = 9$, $p = 0.0002$), and 450.1 ± 98.4% ($n = 9$, $p = 0.001$) increases in sEPSC frequency, respectively (Fig. 2*G*). On the other hand, 100, 300, and 1000 nM orexin B application increased sEPSC frequency to 219.7 ± 66.4% ($n = 9$, $p = 0.35$), 574.0 ± 177.1% ($n = 9$, $p = 0.0006$), and 728.2 ± 161.0% ($n = 9$, $p < 0.0001$) of the control value, respectively (Fig. 2*H*). [Ala^{11}]-Orexin B, an OX2R-selective agonist, also significantly increased sEPSCs in orexin neurons (supplemental Fig. 1, available at www.jneurosci.org as supplemental material). Although the interevent interval was shortened by application of [Ala^{11}]-orexin B (1 μM), the amplitude was not affected [Kolmogorov–Smirnov test: amplitude, [Ala^{11}]-orexin B (1 μM) (p=0.9); interevent interval, [Ala^{11}]-orexin B (1 μM) ($p < 0.001$) (supplemental Fig. 1*B*,*C*, available at www.jneurosci.org as supplemental material)]. [Ala^{11}]-Orexin B (1 μM) increased sEPSC frequency in orexin neurons by 253.0 ± 38.9% ($n = 12$, $p < 0.0001$) (supplemental Fig. 1*D*, available at www.jneurosci.org as supplemental material). Orexin B induced comparable increases in sEPSCs to orexin A. In addition, an OX2R-selective agonist increased sEPSCs. These results might suggest an involvement of OX2R in orexin-induced increases in sEPSC frequency in orexin neurons.

Orexin application had little effect on sIPSC frequency in orexin neurons

The effect of orexin on sIPSCs in orexin neurons was studied as well. sIPSCs were recorded in the presence of AP5 (50 μM) and CNQX (20 μM) at a holding potential of −10 mV. In this recording condition, sIPSCs were recorded as an outward current because the reversal potential of the chloride ion in this recording condition is −74 mV. The outward current was completely abolished by adding PTX (400 μM) in the extracellular solution (data not shown). Orexin B application did not affect sIPSC in the orexin neurons (Fig. 3*A*). sIPSC frequency after application of orexin B at 100, 300, and 1000 nM was 144.4 ± 15.9% ($n = 8$, $p = 0.8$), 93.0 ± 18.4% ($n = 8$, $p = 0.9$), and 168.4 ± 16.9% ($n = 8$, $p = 0.6$) (Fig. 3*B*), respectively. These results suggest that orexin had little effect on GABAergic neurons that directly innervate orexin neurons in the slice preparation.

Orexin-induced activation of orexin neurons is mediated through OX2R

To determine the receptor subtype involved in orexin-induced depolarization of orexin neurons, we used OX1R and OX2R

Table 1. Basic membrane properties of orexin neurons in the *orexin/EGFP*, *OE-OX1R*$^{-/-}$, and *OE-OX2R*$^{-/-}$ mice

	Orexin/EGFP ($n = 10–20$)	*OE-OX1R*$^{-/-}$ ($n = 10–24$)	*OE-OX2R*$^{-/-}$ ($n = 13–35$)
Number of orexin-ir neurons	620 ± 148 ($n = 4$)	682 ± 88 ($n = 4$)	583 ± 78 ($n = 4$)
Capacitance (pF)	24.0 ± 2.5	27.6 ± 2.1	24.0 ± 1.0
Resting membrane potential (mV)	−60.1 ± 1.0	−59.8 ± 1.1	−59.2 ± 2.2
Membrane resistance (MΩ)	579.3 ± 28.0	592.5 ± 34.8	546.0 ± 27.8
Spontaneous firing frequency (Hz)	2.3 ± 0.3	2.3 ± 0.3	2.6 ± 0.2
Action potential peak	29.0 ± 2.4	28.6 ± 3.2	29.3 ± 2.2
Action potential amplitude	61.2 ± 3.2	61.8 ± 3.5	62.8 ± 2.9
Half-width (ms)	4.0 ± 0.4	3.5 ± 0.4	3.3 ± 0.3
sEPSC frequency (Hz)	4.5 ± 0.8	4.1 ± 0.8	3.5 ± 0.5
sEPSC amplitude (pA)	28.9 ± 1.4	27.1 ± 1.2	32.5 ± 3.1
sIPSC frequency (Hz)	1.7 ± 0.3	1.1 ± 0.3	1.1 ± 0.2
sIPSC amplitude (pA)	17.3 ± 0.9	21.5 ± 1.5	18.5 ± 1.6

All parameters were determined by whole-cell slice patch-clamp recordings from orexin neurons with the exception of the number of orexin-ir neurons and spontaneous firing frequency. The number of orexin-ir neurons was counted in every fourth coronal brain section (40 μm) throughout the entire brain. The spontaneous firing frequency was determined by loose cell-attached recordings.

knock-out mice. These orexin receptor knock-out mice were bred with *orexin/EGFP* mice to obtain *orexin/EGFP*;*OX1R*$^{-/-}$ (*OE-OX1R*$^{-/-}$) mice and *orexin/EGFP*;*OX2R*$^{-/-}$ (*OE-OX2R*$^{-/-}$) mice in which orexin neurons express EGFP and an alternative orexin receptor gene (OX1R or OX2R) is knocked out throughout the whole body. The basic membrane properties of orexin neurons in *OE-OX1R*$^{-/-}$ and *OE-OX2R*$^{-/-}$ mice were not significantly different (Table 1) and corroborated previous reports (Yamanaka et al., 2003a; Muraki et al., 2004). The input resistance was calculated from the slope of the current–voltage relationship obtained by step current injection in current-clamp mode. On the other hand, spontaneous firing was determined by loose cell-attached recordings. We found that orexin neurons in *OE-OX1R*$^{-/-}$ mice showed comparable depolarization with orexin neurons in *orexin/EGFP* mice by application of orexin B (1 μM) (6.5 ± 1.1 mV, $n = 9$, $p = 0.11$ vs *orexin/EGFP* mice) (Fig. 4*A*,*B*). The percentage of orexin-responsive orexin neurons in the *OE-OX1R*$^{-/-}$ mice was not different from that in *orexin/EGFP* mice. Twenty-one of twenty-nine orexin neurons in the *OE-OX1R*$^{-/-}$ mice showed depolarization or inward current by orexin B application in the presence of TTX (72.4%). However, orexin neurons in *OE-OX2R*$^{-/-}$ mice completely failed to depolarize with application of orexin B (1 μM) (0.27 ± 0.6 mV, $n = 11$, $p < 0.0001$ vs *orexin/EGFP* mice) (Fig. 4*A*,*B*). We used serotonin (5-HT) as a positive control because previous results demonstrated that 5-HT hyperpolarized all orexin neurons by the activation of G-protein-coupled inwardly rectifying potassium channel via a 5-HT1A receptor (Muraki et al., 2004). All orexin neurons hyperpolarized by 5-HT application failed to respond to orexin B application. These results strongly suggest that OX2R is the primary receptor that is involved in both orexin A- and B-induced depolarization in orexin neurons.

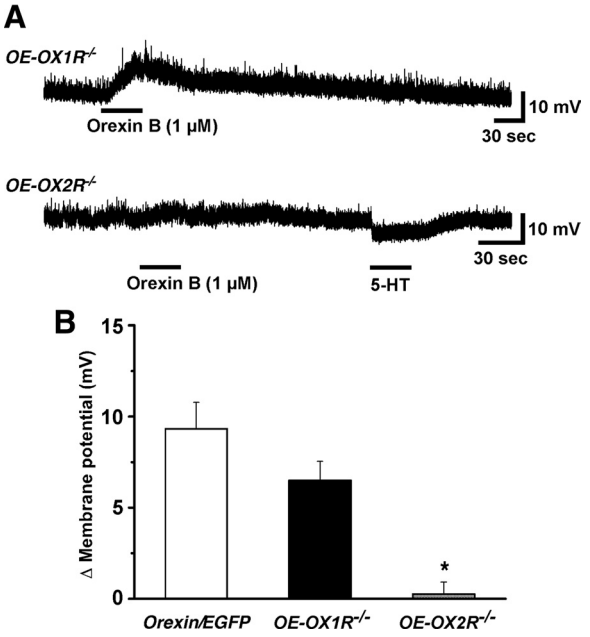

Figure 4. Orexin-induced depolarization of orexin neurons is mediated through OX2R. Orexin neurons in the *OE-OX1R*$^{-/-}$ mice were significantly depolarized by the application of orexin B (1 μM) (***A***, top). However, orexin B failed to depolarize orexin neurons in the *OE-OX2R*$^{-/-}$ mice (***A***, bottom). Orexin B and 5-HT (10 μM) were locally applied during the period represented by the bars. ***B***, Bar graph summarizes the results from ***A***. *$p < 0.05$ versus *orexin/EGFP*. Values are mean ± SEM ($n = 9–10$).

An increase in sEPSCs was mediated through the OX2R

To identify which orexin receptor subtype is involved in orexin-induced increases in sEPSCs in orexin neurons, *OE-OX1R*$^{-/-}$ and *OE-OX2R*$^{-/-}$ mice were used. Basal sEPSC frequency and amplitude in orexin neurons in *OE-OX1R*$^{-/-}$ and *OE-OX2R*$^{-/-}$ mice were slightly lower than those in *orexin/EGFP* mice but were not significantly different (Table 1). Application of orexin B (1 μM) significantly increased sEPSC frequency in the *OE-OX1R*$^{-/-}$ mice to 483.2 ± 73.0% of the control value ($n = 12$, $p < 0.0001$ vs control) (Fig. 5*A*,*E*,*G*). This value was not significantly different from that in *orexin/EGFP* mice ($p = 0.4$ vs *orexin/EGFP*) (Fig. 5*G*). Although interevent interval of sEPSC was significantly shortened, amplitude was not affected by orexin B application [Kolmogorov–Smirnov test: amplitude, orexin B ($p = 0.9$); interevent interval, orexin B ($p < 0.001$) (Fig. 5*C*,*E*)]. However, orexin B (1 μM) failed to increase sEPSCs in the *OE-OX2R*$^{-/-}$ mice (129.3 ± 17.5%) (Fig. 5*B*) ($n = 13$, $p = 0.07$ vs control). Amplitude and frequency were not significantly increased in these mice [Kolmogorov–Smirnov test: amplitude, orexin B ($p = 0.9$); interevent interval, orexin B ($p = 0.7$) (Fig. 5*D*,*F*)]. These results strongly suggest that orexin-induced increases in both sEPSCs were mediated primarily through the OX2R.

Activation of nonselective cation channel is involved in orexin-induced activation of orexin neurons

Membrane resistance was decreased after orexin application, which indicated opening channels downstream of OX2R (Fig. 1*A*,*B*). In addition, orexin B induced inward currents in orexin neurons in the presence of TTX (Fig. 1*C*). To examine the prop-

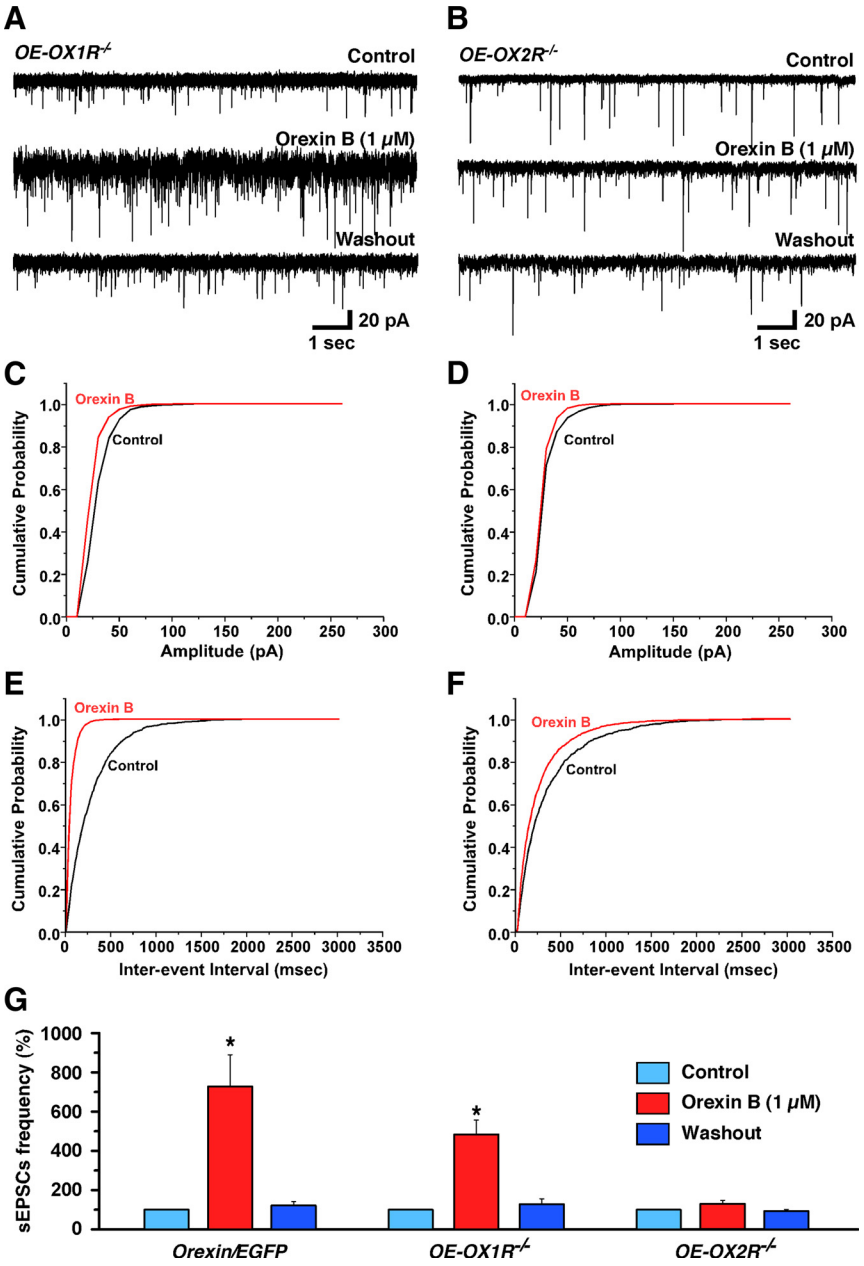

Figure 5. Orexin-induced increases in sEPSCs were mediated through OX2R. sEPSCs were recorded in the presence of PTX (400 μM) at a holding potential of −60 mV. ***A***, Orexin B (1 μM) increased sEPSC frequency in orexin neurons in the *OE-OX1R*$^{-/-}$ mice. ***B***, Orexin B (1 μM) failed to increase sEPSCs in orexin neurons in the *OE-OX2R*$^{-/-}$ mice. ***C***, ***D***, Orexin B (1 μM) did not change sEPSC amplitude in *OE-OX1R*$^{-/-}$ and *OE-OX2R*$^{-/-}$ mice. ***E***, ***F***, Orexin B (1 μM) shortened the interevent interval in *OE-OX1R*$^{-/-}$ mice but not *OE-OX2R*$^{-/-}$ mice. ***G***, Bar graph summarizes the results from ***A*** and ***B***. *$p < 0.05$ versus control. Values are mean ± SEM ($n = 9$–13).

erties of orexin-induced currents in more detail, further electrophysiological experiments were performed. First, we removed calcium from the extracellular solution, Because we have previously reported that cholecystokinin (CCK)-induced, arginine vasopressin (AVP)-induced, and oxytocin-induced inward currents in orexin neurons are significantly increased in calcium-free extracellular solution. The removal of extracellular calcium ions markedly potentiated the orexin-induced inward currents (Fig. 6*A*,*B*). In the presence and absence of calcium ions in the extracellular solution, orexin B (1 μM)-induced inward currents were 30.9 ± 4.6 pA ($n = 6$) and 99.0 ± 25.9 pA ($n = 8$, $p < 0.03$ vs in the presence of calcium ion, unpaired *t* test), respectively. The orexin B-induced inward currents increased ~3.2-fold in calcium-free solution, suggesting that the orexin B-induced inward currents were suppressed by extracellular calcium ions. The reversal potential of the orexin B-induced currents in the calcium-free extracellular solution (in mM: 140 NaCl, 2 CsCl, 1 $MgCl_2$, 1 EGTA, 10 HEPES, 10 glucose, and 10 tetraethyl ammonium chloride) was near 0 mV (0.93 ± 1.4 mV, $n = 6$) when measured with a CsCl pipette solution (in mM: 145 CsCl, 1 $MgCl_2$, 10 HEPES, 1.1 EGTA, and 0.5 Na_2GTP) (Fig. 6*C*). This reversal potential is consistent with the activation of nonselective cation channels in orexin B-induced depolarization of orexin neurons. Several recent reports suggest that the transient receptor potential (TRP) channels play an important role in the receptor-operated influx of cations (Spassova et al., 2004; Takai et al., 2004). In addition, the current through TRP channels has been shown to be suppressed by the presence of extracellular calcium ions (Lintschinger et al., 2000; Hill, 2001). Thus, the activation of the TRP channel downstream of OX2R activation might be involved.

Orexin neurons make a synapse-like contact structure directly on orexin neurons

Orexin neurons are sparsely distributed in the lateral hypothalamic area, and it is unclear whether they make direct connections among orexin neurons. The observations that orexin neurons express functional OX2Rs, their activity is positively modulated by orexin, and they also release glutamate as a neurotransmitter lead us to suppose that they might establish a contact structure similar to that of other chemical synapses to form a positive-feedback circuitry between orexin neurons. To explore this possibility, we took advantage of *orexin/EGFP*;*orexin/haloR*::*GFP* double transgenic mice (supplemental Fig. 2, available at www.jneurosci.org as supplemental material), in which GFP-tagged haloR and EGFP are selectively expressed in orexin neurons; thus, their entire cell morphology can be visualized by immunolabeling for GFP. It should be noted that almost all orexin-immunoreactive (orexin-ir) neurons specifically expressed both haloR::GFP and EGFP and that there was no ectopic expression of GFP other than orexin-ir neurons (supplemental Fig. 2*B*, available at www.jneurosci.org as supplemental material). We found that the immunoreactivity for orexin (Fig. 7*A*,*B*) or EGFP (GFP-ir) (Fig. 7*C*,*D*) allowed the successful visualization of orexin neurons and revealed a close apposition between immunopositive axons and dendrites or somata in the lateral hypothalamus (Fig. 7*A*–*D*, arrows). The visualization of GFP-ir axons was much clearer than orexin-ir axons,

which might be because of the homogeneous distribution of haloR and EGFP in the plasma membrane and cytoplasm of orexin neurons, respectively. For this reason, an anti-GFP antibody was used for the following electron microscopic observations. At the electron microscopic level, GFP-ir was identified by the presence of electron-dense DAB reaction end products. GFP-ir axon fibers were found to form synapse-like contacting structures on GFP-ir cell bodies and dendritic processes where the plasma membrane of cell body/dendrite was accompanied by electron-dense matrix just beneath the contact (Fig. 7*E–H*). At the contacting site, the GFP-ir axon fibers showed an enlargement in diameter, making a varicosity-like structure (Fig. 7*F*,*G*,*I*,*J*). We observed a few large vesicles (~100 nm in diameter) and some small clear vesicles (~50 nm in diameter) within the varicosity (Fig. 7*F*). An example of the contact between a GFP-ir axon and a GFP-ir dendrite was illustrated in a three-dimensional reconstruction obtained from serial sections including those shown in Figure 7, *G* and *H* (Fig. 7*I*,*J*; see also supplemental Fig. 3, available at www.jneurosci.org as supplemental material, showing three-dimensional animation of this profile). These electron microscopic observations suggest that orexin neurons communicate with each other, at least in part, at the close apposition site.

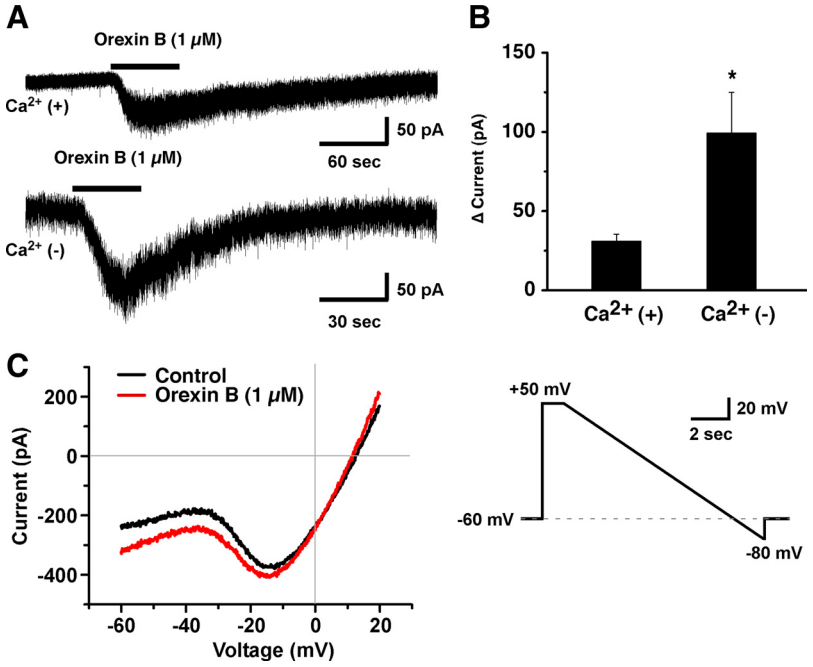

Figure 6. Orexin activated orexin neurons by opening nonselective cation channels in orexin neurons. ***A***, The effect of extracellular Ca^{2+} on orexin B (1 μM)-induced inward currents. Orexin B induced weak inward currents in the presence of extracellular calcium (Ca^{2+}) (top). This inward current was dramatically increased in the Ca^{2+} free solution (bottom). ***B***, The Ca^{2+}-free solution caused threefold increases in inward current. ***C***, The current–voltage relationship obtained by voltage ramp protocol using a CsCl pipette in the Ca^{2+}-free extracellular solution is shown. The *I–V* curve shows that the reversal potential of the orexin B (1 μM)-induced currents was 0.93 ± 1.4 mV ($n = 6$). Neurons were voltage clamped at −60 mV, and the membrane potential was stepped to 50 mV (1 s), and then ramped to −80 mV at duration of 10 s (right). Orexin B was locally applied during the period represented by the bars. *$p < 0.05$ versus Ca^{2+}(+). Values are mean ± SEM ($n = 6–8$).

Orexin neurons in *OE-OX2R*$^{-/-}$ mice completely failed to respond to orexin

To further investigate the physiological role of orexin-induced activation of orexin neurons, the spontaneous activity of orexin neurons was recorded by using a loose cell-attached recording in the brain slice preparation. Loose cell-attached recordings revealed that the spontaneous firing rate of orexin neurons is not significantly different between *orexin/EGFP*, *OE-OX1R*$^{-/-}$, and *OE-OX2R*$^{-/-}$ mice (Table 1). Spontaneous firing is not affected in the presence of PTX (2.64 ± 0.40 Hz, $n = 8$) or AP5, CNQX, and PTX (2.47 ± 0.37 Hz, $n = 9$). The local application of orexin B (1 μM) significantly increased the firing rate to 223.2 ± 39.3% ($n = 10$, $p = 0.0002$) of the control value in the orexin neurons in *orexin/EGFP* mice (Fig. 8*A–C*). After orexin B local application, the firing rate gradually increased and reached a maximum response ~1 min after application. Furthermore, the increase in firing lasted for a few minutes (3–6 min) after washout. Orexin-induced increases in firing rate were not inhibited in the presence of PTX alone or APV, CNQX, and PTX. In the presence of PTX alone or APV, CNQX, and PTX, application of orexin B (1 μM) increased the firing rate to 216.4 ± 43.0% ($n = 8$, $p = 0.004$) or 153.5 ± 14.7% ($n = 9$, $p = 0.006$ vs control), respectively (Fig. 8*C*). Orexin neurons in the *OE-OX1R*$^{-/-}$ mice showed equally potent increases in firing by the application of orexin B (1 μM) compared with *orexin/EGFP* mice (257 ± 42.4%; $n = 21$, $p < 0.001$ vs control). However, orexin neurons in the *OE-OX2R*$^{-/-}$ mice completely failed to respond to orexin B (1 μM, 101.3 ± 2.3%, $n = 21$, $p = 0.29$). These results suggest that orexin signaling through OX2R has a crucial role in the regulation of the activity of orexin neurons.

Discussion

In the present study, we demonstrated that orexin neurons are directly and indirectly activated by orexin. Slice patch-clamp recordings from orexin neurons in orexin receptor knock-out mice revealed that both direct and indirect activations of orexin neurons are mediated through OX2R. Immunoelectron microscopic analyses showed direct interaction between orexin neurons.

OX2R is involved in both direct and indirect activation of orexin neurons

Li et al. (2002) reported that orexin A (hypocretin-1; 2 μM) indirectly activated orexin neurons through increasing sEPSCs in orexin neurons, but orexin A failed to activate in the presence of glutamatergic synaptic transmission blockers ($n = 7$), AP5 (50 μM) and CNQX (10 μM). However, in the present study, orexin B (1 μM)-induced activation was observed not only in the presence of TTX (1 μM), but also in the presence of TTX (1 μM), AP5 (50 μM), and CNQX (20 μM) (Fig. 1*G*). In addition, orexin B induced inward currents in the presence of TTX (Fig. 1*C*). These results strongly suggest that orexin directly activates orexin neurons. The discordance in the studies may be procedural in terms of the number of experiments conducted and the application of orexin. We studied large numbers of orexin neurons (149 neurons). However, some orexin neurons in *orexin/EGFP* mice failed to respond to orexin (23%, 34 of 149), and the effect of orexin was obviously diminished in the second application. For these reasons, we replaced the brain slice preparation in each experiment.

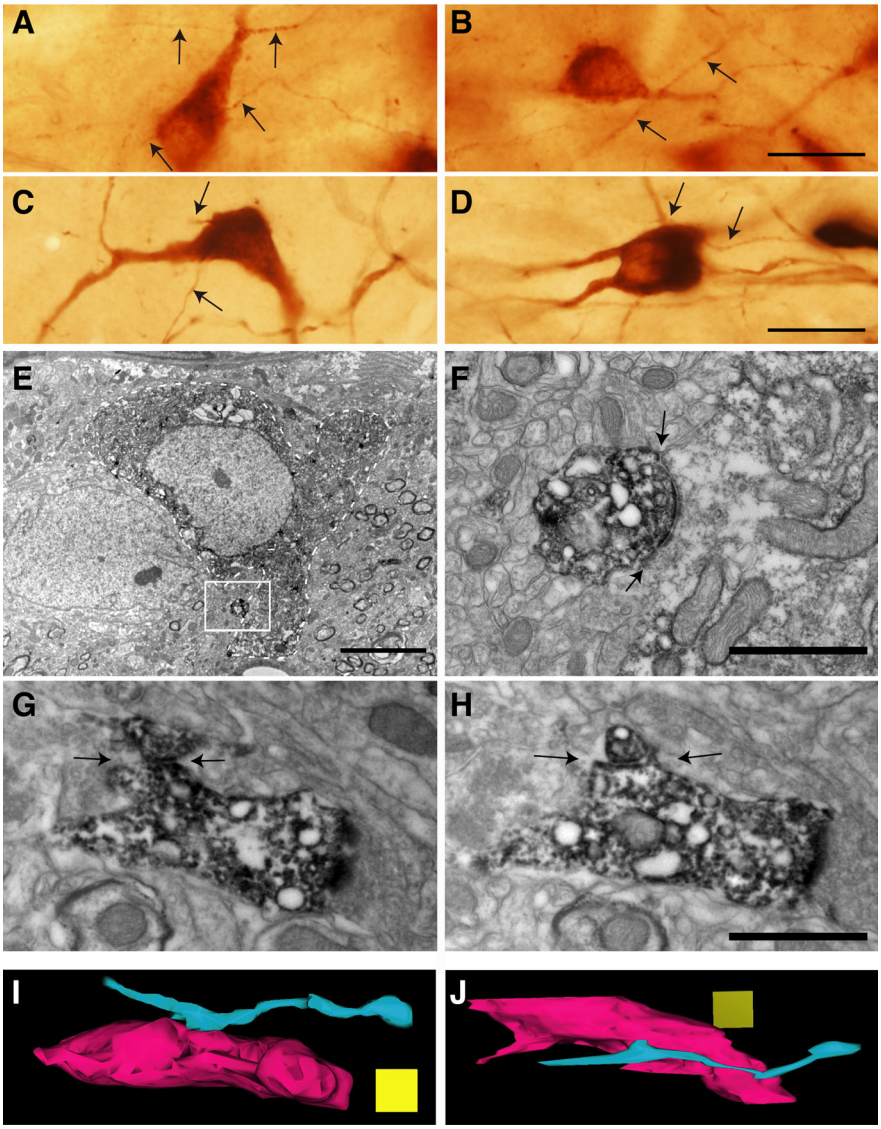

Figure 7. Immunoelectron microscopic observation revealed synapse-like close appositions between the axon and the dendrite of orexin neurons. ***A–D***, Light-microscopic images of DAB-labeled orexin neurons. Orexin neurons were labeled with anti-orexin antibody (***A***, ***B***) or anti-GFP antibody (***C***, ***D***) in *orexin/EGFP;orexin/haloR::GFP* double transgenic mice in which orexin neurons specifically express EGFP and haloR::GFP. The axons of orexin neurons were in close apposition with a dendrite or soma from other orexin neurons in many regions in the hypothalamus (arrows). ***E–H***, Immunoelectron microscopy of the apposition sites between GFP-ir axons and a GFP-ir soma or dendrite (orexin neuron). ***F***, Magnification of the square region in ***E***. Arrows indicate a contacting zone of two GFP-ir positive profiles, where two plasma membranes align in parallel (***F–H***). Note that the plasma membranes of GFP-ir profiles shows thickening of the plasma membrane selectively at the contacting site. ***I***, ***J***, Three-dimensional reconstruction of two GFP-ir profiles from serial sections including ***G*** and ***H***. A bulge structure appeared at where an axon of an orexin neuron contacted a dendrite of another orexin neuron. Scale bars: ***A–D***, 20 μm; ***E***, 5 μm; ***F–H***, 1 μm. Scale cube: ***I***, ***J***, 0.7^3 μm^3.

Our results suggest that OX2R is involved in the orexin activation of orexin neurons: orexin A and B induced comparable depolarization; an OX2R-specific agonist, [Ala^{11}]-orexin B, induced depolarization; and orexin neurons in the *OE-OX2R*$^{-/-}$ mice completely failed to respond to orexin B. This suggests that orexin neurons express functional OX2Rs, and orexin activates orexin neurons through the OX2R. Orexin B (hypocretin-2)-saporin injection into the lateral hypothalamic area decreased the number of orexin neurons and histaminergic neurons (Gerashchenko et al., 2001), corroborating our results. Orexin B-saporin injection ablated orexin neurons via the OX2R expressed in orexin neurons. The reversal potential of the orexin-induced current was near 0 mV (0.93 ± 1.4 mV, $n = 6$). This suggests the activation of nonselective cation channels downstream of OX2R. The activation of phospholipase C by the $\beta\gamma$ subunit of the G-protein might be involved because OX2R is believed to couple with the Gq and Gi types of G-proteins (Zhu et al., 2003). We previously showed that orexin neurons are activated by CCK and AVP via the G-protein-coupled receptors (Gq), CCK_A receptor, and the V1a receptor (Tsujino et al., 2005; Tsunematsu et al., 2008). Both CCK- and AVP-induced inward currents were robustly enhanced by removing the calcium ions from the extracellular solution. The orexin-induced inward current was also enhanced in the calcium-free solution (Fig. 6), suggesting the involvement of the same type of nonselective cation channels, which are likely TRP channels, because the CCK- and AVP-induced currents were inhibited by the TRP channel blocker SKF96365 (Tsujino et al., 2005; Tsunematsu et al., 2008). It has been reported that orexin-induced depolarization is mediated through the Na^+/Ca^{2+} exchanger in arcuate and TMN neurons (Eriksson et al., 2001; Burdakov et al., 2003). To study the involvement of this exchanger in orexin-induced depolarization in orexin neurons, BAPTA (10 mM) was added to the pipette solution. However, orexin-induced depolarization of orexin neurons was not inhibited by adding BAPTA to the pipette solution, suggesting that the Na^+/Ca^{2+} exchanger is not involved in orexin-induced depolarization of orexin neurons via the OX2R.

Physiological significance of orexin-induced activation of orexin neurons via OX2R

Prepro-orexin and OX2R knock-out mice, in addition to OX2R-mutated dogs, have been shown to display various phenotypes: fragmentation of sleep/wakefulness cycle, direct transition from awake to REM sleep, and suddenly triggered behavioral arrest (cataplexy) (Lin et al., 1999; Willie et al., 2003). These are strikingly similar to the symptoms observed in narcolepsy. However, OX1R knock-out mice showed mild or almost no abnormality in sleep/wakefulness, which suggests that OX2R has a critical role in the regulation of sleep/wakefulness. Why does this difference in phenotype arise? The differential expression patterns of OX1R and OX2R might be a clue to answering this question. OX1R is densely expressed in the locus ceruleus, dorsomedial nucleus of hypothalamus, and paraventricular nucleus. On the other hand, OX2R is densely expressed in the cerebral cortex, septal nuclei, hippocampus, and hypothalamic nuclei, including the histaminergic tuberomammillary nucleus (TMN) (Marcus et al., 2001). Among these brain regions, the TMN is thought to be the center for the site of action of orexin-induced arousal. Because histaminergic TMN neurons are implicated in arousal (Lin et al., 1988; Monti, 1993), they fire

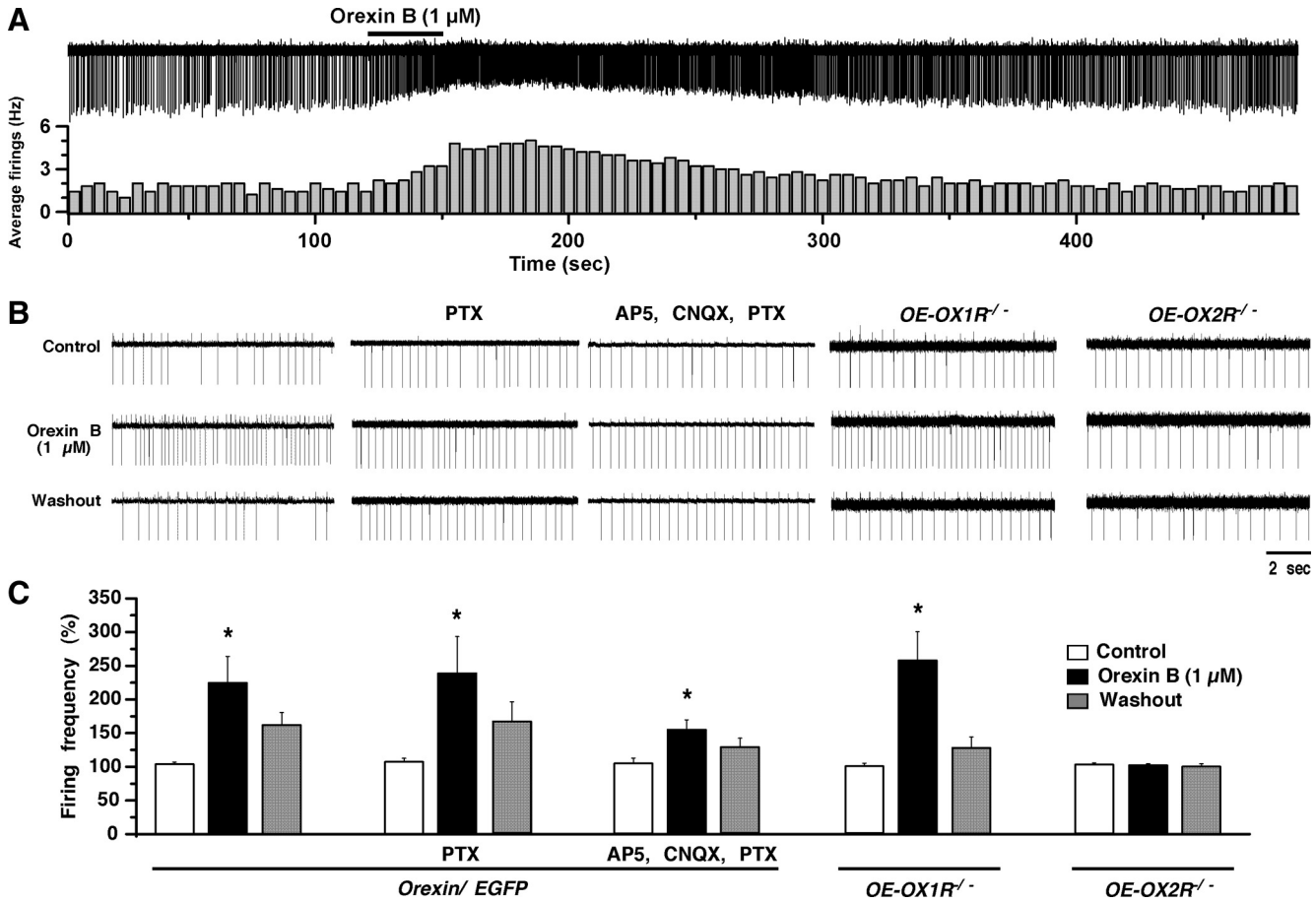

Figure 8. Loose cell-attached recordings revealed that orexin neurons in the *OE-OX2R*$^{-/-}$ mice completely failed to respond to orexin. ***A***, Representative trace (top) shows that orexin B application increased firing in orexin neurons in the *orexin/EGFP* mice. Bar graph (bottom) shows an average firing for every 5 s. ***B***, Application of orexin B (1 μM) increased firing in orexin neurons in the *orexin/EGFP* and *OE-OX1R*$^{-/-}$ mice. However, application of orexin B (1 μM) completely failed to increase the firing rates of orexin neurons in the *OE-OX2R*$^{-/-}$ mice. ***C***, Bar graph summarizes the results from ***B***. Orexin B was locally applied during the period represented by the bars. The firing increase is indicated as a percentage increase from the basal firing rate (i.e., the average firing for 3 min before the start of the experiment). Control represents the average firing for 1 min before orexin B application. AP5 (50 μM), CNQX (20 μM), and PTX (400 μM) were applied by bath application. *$p < 0.05$ versus control. Values are mean ± SEM ($n = 5$–21).

tonically during wakefulness (Steininger et al., 1999) and are activated by orexin via the OX2R (Bayer et al., 2001; Eriksson et al., 2001; Yamanaka et al., 2002). In addition, the effect of orexin on arousal was not observed in histamine 1 receptor knock-out (*H1*$^{-/-}$) mice (Huang et al., 2001). However, histidine decarboxylase knock-out (*HDC*$^{-/-}$) mice, *H1*$^{-/-}$ mice, and *OX1R*$^{-/-}$;*H1*$^{-/-}$ double knock-out mice did not show severe narcoleptic phenotypes (Anaclet et al., 2009; Hondo et al., 2010), suggesting that downstream pathways of OX2R, other than the histaminergic system, are critical for the regulation of sleep/wakefulness.

Here, we revealed that orexin neurons are directly and indirectly activated by orexin through the OX2R. Immunoelectron microscopic analyses revealed that orexin neurons are directly innervated by orexin neurons. These results suggest that connections between orexin neurons form a positive-feedback circuit. Figure 9 summarizes a schematic model for orexin-induced activation of orexin neurons via the OX2R. This positive-feedback circuitry might function to keep the activity of orexin neurons at a high level while the animals are waking. In current-clamp recording, we found that some orexin neurons showed burst-type firing, and this type of neuron has been shown to fire in clusters or episodes of repetitive bursts (Yamanaka et al., 2003a). This rhythmic firing might work as a pacemaker to maintain orexin neural activity. Orexin-induced increases in sEPSCs were also mediated via OX2R. sEPSC increases in orexin neurons might include input from other orexin neurons because orexin neurons are believed to be glutamatergic. In addition, they are activated by orexin via OX2R.

Interestingly, PTX, AP5, and CNQX had little effect on the basal firing rates of orexin neurons; however, these inhibitors significantly inhibited orexin B-induced increases in firing ($p = 0.014$ vs orexin B alone). This result suggests that orexin neurons have spontaneous firing ability independent from excitatory inputs. This does not deny the contribution of sEPSCs and sIPSCs on the activity of orexin neurons. sEPSCs or sIPSCs additively modulate the activity of orexin neurons at relatively higher firing rates. The orexin neurons in the *OE-OX2R*$^{-/-}$ mice that completely failed to respond to orexin might suggest that the activity of orexin neurons *in vivo* is decreased in *OX2R*$^{-/-}$ mice. This results in a significant decrease in orexin release because orexin is stored in dense-core vesicles and released at a higher firing frequency (Torrealba et al., 2003). This might be one reason that the phenotype of *OX2R*$^{-/-}$ mice was similar to that of *prepro-orexin*$^{-/-}$ mice with regard to sleep/wakefulness regulation. In any case, our results help to clarify how the activity of orexin neurons is regulated *in vivo* and how arousal is maintained by orexin neurons.

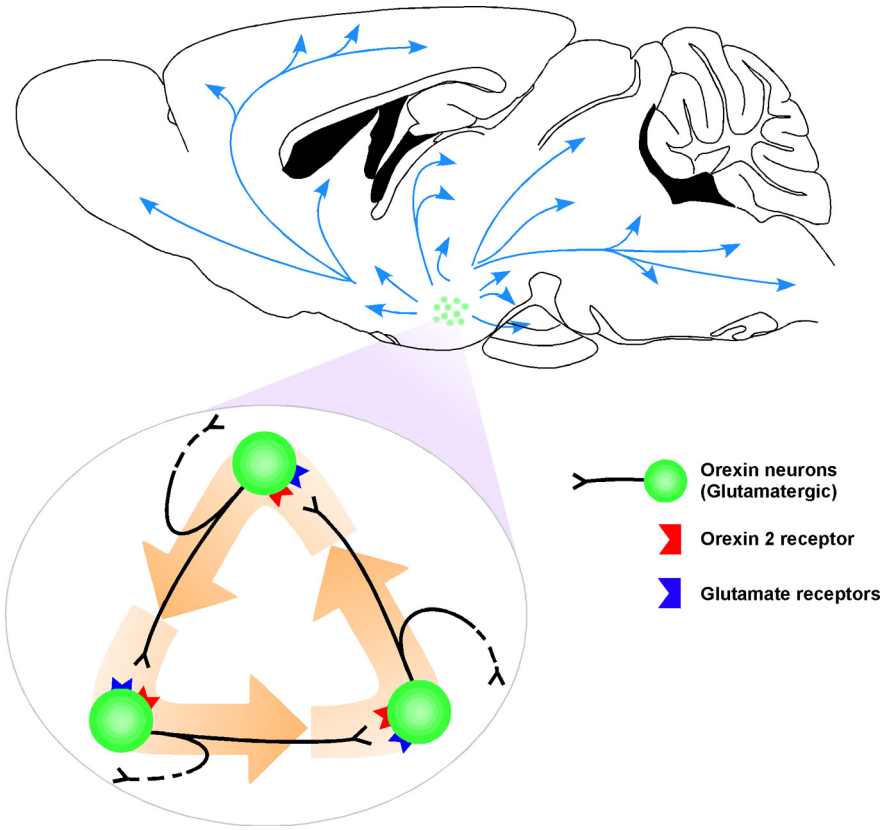

Figure 9. Schematic summarizing the mechanism underlying orexin-induced activation of orexin neurons through OX2R. Orexin neurons directly innervate orexin neurons and activate orexin neurons through OX2R. This might form a positive feedback circuit, and the circuitry might function to preserve the activity of orexin neurons and subsequently to maintain arousal. Glutamate receptors include AMPA, NMDA, and metabotropic glutamate receptors.

Loss of function of OX2R induces not only fragmentation of wake episodes, but also fragmentation of non-REM sleep. It is likely that the OX2R-mediated positive feedback is not directly involved in the fragmentation of non-REM sleep because orexin neurons are thought to be almost silent during non-REM sleep (Mileykovskiy et al., 2005). However, the positive feedback between orexin neurons might indirectly affect non-REM sleep by increasing orexin release during wakefulness. An increase in orexin concentration in the CSF might contribute to consolidating wakefulness and non-REM sleep because orexin also activates GABAergic neurons that are implicated in the initiation and maintenance of non-REM sleep (Korotkova et al., 2002; Burdakov et al., 2003; Eriksson et al., 2004). After silencing orexin neurons in non-REM sleep, orexin in the CSF might activate GABAergic neurons and increase IPSCs in neurons that are responsible for arousal, such as the TMN neurons (Eriksson et al., 2004).

Our study suggests that orexin neurons form a positive-feedback circuit between orexin neurons. This circuitry might be important for maintaining the activity of orexin neurons at a high level and/or for lasting a long time. We found that not only the direct activation of orexin neurons but also indirect activation through an increase in excitatory input to orexin neurons (by activating glutamatergic neurons) is mediated through the OX2R. This synergistic activation of neurons might be important in amplifying signals for arousal from the brainstem and in the maintenance of arousal. Future experiments using transgenic mice in which the OX2R is specifically knocked out in the orexin neurons may reveal the physiological importance of orexin-induced activation of orexin neurons through the OX2R.

References

Anaclet C, Parmentier R, Ouk K, Guidon G, Buda C, Sastre JP, Akaoka H, Sergeeva OA, Yanagisawa M, Ohtsu H, Franco P, Haas HL, Lin JS (2009) Orexin/hypocretin and histamine: distinct roles in the control of wakefulness demonstrated using knock-out mouse models. J Neurosci 29:14423–14438.

Asahi S, Egashira S, Matsuda M, Iwaasa H, Kanatani A, Ohkubo M, Ihara M, Morishima H (2003) Development of an orexin-2 receptor selective agonist, [Ala(11), D-Leu(15)]orexin-B. Bioorg Med Chem Lett 13:111–113.

Bayer L, Eggermann E, Serafin M, Saint-Mleux B, Machard D, Jones B, Mühlethaler M (2001) Orexins (hypocretins) directly excite tuberomammillary neurons. Eur J Neurosci 14:1571–1575.

Burdakov D, Liss B, Ashcroft FM (2003) Orexin excites GABAergic neurons of the arcuate nucleus by activating the sodium–calcium exchanger. J Neurosci 23:4951–4957.

Chemelli RM, Willie JT, Sinton CM, Elmquist JK, Scammell T, Lee C, Richardson JA, Williams SC, Xiong Y, Kisanuki Y, Fitch TE, Nakazato M, Hammer RE, Saper CB, Yanagisawa M (1999) Narcolepsy in orexin knockout mice: molecular genetics of sleep regulation. Cell 98:437–451.

de Lecea L, Kilduff TS, Peyron C, Gao X, Foye PE, Danielson PE, Fukuhara C, Battenberg EL, Gautvik VT, Bartlett FS 2nd, Frankel WN, van den Pol AN, Bloom FE, Gautvik KM, Sutcliffe JG (1998) The hypocretins: hypothalamus-specific peptides with neuroexcitatory activity. Proc Natl Acad Sci U S A 95:322–327.

Eriksson KS, Sergeeva O, Brown RE, Haas HL (2001) Orexin/hypocretin excites the histaminergic neurons of the tuberomammillary nucleus. J Neurosci 21:9273–9279.

Eriksson KS, Sergeeva OA, Selbach O, Haas HL (2004) Orexin (hypocretin)/dynorphin neurons control GABAergic inputs to tuberomammillary neurons. Eur J Neurosci 19:1278–1284.

Fiala JC (2005) Reconstruct: a free editor for serial section microscopy. J Microsc 218:52–61.

Gerashchenko D, Salin-Pascual R, Shiromani PJ (2001) Effects of hypocretin-saporin injections into the medial septum on sleep and hippocampal theta. Brain Res 913:106–115.

Hara J, Beuckmann CT, Nambu T, Willie JT, Chemelli RM, Sinton CM, Sugiyama F, Yagami K, Goto K, Yanagisawa M, Sakurai T (2001) Genetic ablation of orexin neurons in mice results in narcolepsy, hypophagia, and obesity. Neuron 30:345–354.

Hill B (2001) Ion channels of excitable membranes. Sunderland, MA: Sinauer.

Hondo M, Nagai K, Ohno K, Kisanuki Y, Willie JT, Watanabe T, Yanagisawa M, Sakurai T (2010) Histamine-1 receptor is not required as a downstream effector of orexin-2 receptor in maintenance of basal sleep/wake states. Acta Physiol (Oxf) 198:287–294.

Huang ZL, Qu WM, Li WD, Mochizuki T, Eguchi N, Watanabe T, Urade Y, Hayaishi O (2001) Arousal effect of orexin A depends on activation of the histaminergic system. Proc Natl Acad Sci U S A 98:9965–9970.

Korotkova TM, Eriksson KS, Haas HL, Brown RE (2002) Selective excitation of GABAergic neurons in the substantia nigra of the rat by orexin/hypocretin in vitro. Regul Pept 104:83–89.

Li Y, Gao XB, Sakurai T, van den Pol AN (2002) Hypocretin/orexin excites hypocretin neurons via a local glutamate neuron: a potential mechanism for orchestrating the hypothalamic arousal system. Neuron 36:1169–1181.

Lin JS, Sakai K, Jouvet M (1988) Evidence for histaminergic arousal mechanisms in the hypothalamus of cat. Neuropharmacology 27:111–122.

Lin L, Faraco J, Li R, Kadotani H, Rogers W, Lin X, Qiu X, de Jong PJ, Nishino S, Mignot E (1999) The sleep disorder canine narcolepsy is caused by a mutation in the hypocretin (orexin) receptor 2 gene. Cell 98:365–376.

Lintschinger B, Balzer-Geldsetzer M, Baskaran T, Graier WF, Romanin C, Zhu MX, Groschner K (2000) Coassembly of Trp1 and Trp3 proteins generates diacylglycerol- and Ca2+-sensitive cation channels. J Biol Chem 275:27799–27805.

Marcus JN, Aschkenasi CJ, Lee CE, Chemelli RM, Saper CB, Yanagisawa M, Elmquist JK (2001) Differential expression of orexin receptors 1 and 2 in the rat brain. J Comp Neurol 435:6–25.

Mileykovskiy BY, Kiyashchenko LI, Siegel JM (2005) Behavioral correlates of activity in identified hypocretin/orexin neurons. Neuron 46:787–798.

Monti JM (1993) Involvement of histamine in the control of the waking state. Life Sci 53:1331–1338.

Muraki Y, Yamanaka A, Tsujino N, Kilduff TS, Goto K, Sakurai T (2004) Serotonergic regulation of the orexin/hypocretin neurons through the 5-HT1A receptor. J Neurosci 24:7159–7166.

Nambu T, Sakurai T, Mizukami K, Hosoya Y, Yanagisawa M, Goto K (1999) Distribution of orexin neurons in the adult rat brain. Brain Res 827:243–260.

Sakurai T, Amemiya A, Ishii M, Matsuzaki I, Chemelli RM, Tanaka H, Williams SC, Richardson JA, Kozlowski GP, Wilson S, Arch JRS, Buckingham RE, Haynes AC, Carr SA, Annan RS, McNulty DE, Liu W-S, Terrett JA, Elshourbagy NA, Bergsma DJ, et al. (1998) Orexins and orexin receptors: a family of hypothalamic neuropeptides and G protein-coupled receptors that regulate feeding behavior. Cell 92:573–585.

Sakurai T, Moriguchi T, Furuya K, Kajiwara N, Nakamura T, Yanagisawa M, Goto K (1999) Structure and function of human prepro-orexin gene. J Biol Chem 274:17771–17776.

Spassova MA, Soboloff J, He LP, Hewavitharana T, Xu W, Venkatachalam K, van Rossum DB, Patterson RL, Gill DL (2004) Calcium entry mediated by SOCs and TRP channels: variations and enigma. Biochim Biophys Acta 1742:9–20.

Steininger TL, Alam MN, Gong H, Szymusiak R, McGinty D (1999) Sleep-waking discharge of neurons in the posterior lateral hypothalamus of the albino rat. Brain Res 840:138–147.

Takai Y, Sugawara R, Ohinata H, Takai A (2004) Two types of non-selective cation channel opened by muscarinic stimulation with carbachol in bovine ciliary muscle cells. J Physiol 559:899–922.

Torrealba F, Yanagisawa M, Saper CB (2003) Colocalization of orexin a and glutamate immunoreactivity in axon terminals in the tuberomammillary nucleus in rats. Neuroscience 119:1033–1044.

Tsujino N, Yamanaka A, Ichiki K, Muraki Y, Kilduff TS, Yagami K, Takahashi S, Goto K, Sakurai T (2005) Cholecystokinin activates orexin/hypocretin neurons through the cholecystokinin A receptor. J Neurosci 25:7459–7469.

Tsunematsu T, Fu LY, Yamanaka A, Ichiki K, Tanoue A, Sakurai T, van den Pol AN (2008) Vasopressin increases locomotion through a V1a receptor in orexin/hypocretin neurons: implications for water homeostasis. J Neurosci 28:228–238.

Willie JT, Chemelli RM, Sinton CM, Tokita S, Williams SC, Kisanuki YY, Marcus JN, Lee C, Elmquist JK, Kohlmeier KA, Leonard CS, Richardson JA, Hammer RE, Yanagisawa M (2003) Distinct narcolepsy syndromes in orexin receptor-2 and orexin null mice: molecular genetic dissection of non-REM and REM sleep regulatory processes. Neuron 38:715–730.

Yamanaka A, Tsujino N, Funahashi H, Honda K, Guan JL, Wang QP, Tominaga M, Goto K, Shioda S, Sakurai T (2002) Orexins activate histaminergic neurons via the orexin 2 receptor. Biochem Biophys Res Commun 290:1237–1245.

Yamanaka A, Muraki Y, Tsujino N, Goto K, Sakurai T (2003a) Regulation of orexin neurons by the monoaminergic and cholinergic systems. Biochem Biophys Res Commun 303:120–129.

Yamanaka A, Beuckmann CT, Willie JT, Hara J, Tsujino N, Mieda M, Tominaga M, Yagami K, Sugiyama F, Goto K, Yanagisawa M, Sakurai T (2003b) Hypothalamic orexin neurons regulate arousal according to energy balance in mice. Neuron 38:701–713.

Zhu Y, Miwa Y, Yamanaka A, Yada T, Shibahara M, Abe Y, Sakurai T, Goto K (2003) Orexin receptor type-1 couples exclusively to pertussis toxin-insensitive G-proteins, while orexin receptor type-2 couples to both pertussis toxin-sensitive and -insensitive G-proteins. J Pharmacol Sci 92:259–266.